

Chronobiology International

The Journal of Biological and Medical Rhythm Research

ISSN: (Print) (Online) Journal homepage: www.tandfonline.com/journals/icbi20

TASK-3, two-pore potassium channels, contribute to circadian rhythms in the electrical properties of the suprachiasmatic nucleus and play a role in driving stable behavioural photic entrainment

Aiste Steponenaite, Tatjana Lalic, Lynsey Atkinson, Neil Tandy, Lorna Brown, Alistair Mathie, Zameel M. Cader & Gurprit S. Lall

To cite this article: Aiste Steponenaite, Tatjana Lalic, Lynsey Atkinson, Neil Tandy, Lorna Brown, Alistair Mathie, Zameel M. Cader & Gurprit S. Lall (17 May 2024): TASK-3, two-pore potassium channels, contribute to circadian rhythms in the electrical properties of the suprachiasmatic nucleus and play a role in driving stable behavioural photic entrainment, Chronobiology International, DOI: [10.1080/07420528.2024.2351515](https://doi.org/10.1080/07420528.2024.2351515)

To link to this article: <https://doi.org/10.1080/07420528.2024.2351515>



© 2024 The Author(s). Published with license by Taylor & Francis Group, LLC.



[View supplementary material](#)



Published online: 17 May 2024.



[Submit your article to this journal](#)



Article views: 68



[View related articles](#)



[View Crossmark data](#)

TASK-3, two-pore potassium channels, contribute to circadian rhythms in the electrical properties of the suprachiasmatic nucleus and play a role in driving stable behavioural photic entrainment

Aiste Steponenaite^{a*}, Tatjana Lalic^{b*}, Lynsey Atkinson^{a*}, Neil Tandy^a, Lorna Brown^a, Alistair Mathie^a, Zameel M. Cader^b, and Gurprit S. Lall^{a*}

^aMedway School of Pharmacy, University of Kent, Kent, UK; ^bTranslational Molecular Neuroscience Group, University of Oxford, Oxford, UK

ABSTRACT

Stable and entrainable physiological circadian rhythms are crucial for overall health and well-being. The suprachiasmatic nucleus (SCN), the primary circadian pacemaker in mammals, consists of diverse neuron types that collectively generate a circadian profile of electrical activity. However, the mechanisms underlying the regulation of endogenous neuronal excitability in the SCN remain unclear. Two-pore domain potassium channels (K2P), including TASK-3, are known to play a significant role in maintaining SCN diurnal homeostasis by inhibiting neuronal activity at night. In this study, we investigated the role of TASK-3 in SCN circadian neuronal regulation and behavioural photoentrainment using a TASK-3 global knockout mouse model. Our findings demonstrate the importance of TASK-3 in maintaining SCN hyperpolarization during the night and establishing SCN sensitivity to glutamate. Specifically, we observed that TASK-3 knockout mice lacked diurnal variation in resting membrane potential and exhibited altered glutamate sensitivity both in vivo and in vitro. Interestingly, despite these changes, the mice lacking TASK-3 were still able to maintain relatively normal circadian behaviour.

ARTICLE HISTORY

Received 24 August 2023
Revised 20 March 2024
Accepted 19 April 2024

KEYWORDS

SCN; TASK-3; background two-pore domain potassium channels (K2P); entrainment; resting membrane potential; circadian rhythms

Introduction

The suprachiasmatic nucleus (SCN) is a group of neurons that function as the circadian master clock in mammals, enabling us to adapt to environmental rhythms and regulate our daily lives. This autonomous clock operates under the control of multiple transcription translation feedback loops (TTFL) with CLOCK and BMAL1 proteins being the initiators of the cascade of transcriptional events occurring at the nucleus (Patton and Hastings 2018; Takahashi 2017). While light provides the strongest synchronizing cue to the circadian clock, the cycles of gene expression and electrical activity in the suprachiasmatic nucleus can occur in the absence of light (Welsh et al. 2010).

Despite neuronal heterogeneity, there is a clear pattern of electrical activity where SCN neurons generate high frequency action potentials during the day, which are silenced during the night (Allen et al. 2017). K⁺ dependent conductance hyperpolarizes membranes, rendering cells electrically inactive. Daily depolarization is mainly maintained by voltage gated Na⁺ and Ca²⁺ channels together with

hyperpolarization activated cyclic nucleotide gated channels and NALCN sodium leak channel, bringing the membranes to a more depolarized state and placing them near the threshold for generating an action potential (Allen et al. 2017; Patton and Hastings 2018). At night, hyperpolarizing K⁺ dependent conductance acts to inactivate neurons, with contribution from calcium-activated K⁺ (BK) channels (Meredith et al. 2006).

Background two-pore domain potassium channels (K2P) play a major role in hyperpolarization by providing a leak K⁺ current over a wide voltage range (Felicangeli et al. 2015; Renigunta et al. 2015). Several of these 15 K2P channels, such as TRESK, TASK-1, TASK-3 and TRAAK, are known to be expressed in the suprachiasmatic nucleus (SCN) (Lalic et al. 2020; Talley et al. 2001). Recently, we showed that the background two-pore domain potassium channel TRESK plays an essential part in SCN regulation, through glutamate and calcium signalling (Lalic et al. 2020). However, the role of TASK-3 in the SCN and circadian rhythms remains unclear.

CONTACT Gurprit S. Lall  G.Lall@kent.ac.uk  Medway School of Pharmacy, University of Kent, Anson Building, Central Avenue, Chatham, Kent ME4 4TB, UK

*These authors contributed equally to this work.

 Supplemental data for this article can be accessed online at <https://doi.org/10.1080/07420528.2024.2351515>

© 2024 The Author(s). Published with license by Taylor & Francis Group, LLC.

This is an Open Access article distributed under the terms of the Creative Commons Attribution-NonCommercial-NoDerivatives License (<http://creativecommons.org/licenses/by-nc-nd/4.0/>), which permits non-commercial re-use, distribution, and reproduction in any medium, provided the original work is properly cited, and is not altered, transformed, or built upon in any way. The terms on which this article has been published allow the posting of the Accepted Manuscript in a repository by the author(s) or with their consent.

TASK-3 is encoded by the *kcnk9* gene, also known as $K_{2p9.1}$. It is expressed in the brain, with very high expression in the suprachiasmatic nucleus, peripheral organs, such as the retina, breast and lung (Brickley et al. 2007; Sans et al. 2000; Sun et al. 2016; Talley et al. 2001). The Human Brain Atlas data on TASK-3 (KCNK9) shows high expression levels in mouse hypothalamus (27.8 nTPM). Single cell type expression data shows high TASK-3 expression in excitatory (15.4 nTPM) as well as inhibitory (7.6 nTPM) neurons, whereas the expression in astrocytes is relatively low (0.6 nTPM, Single cell type – KCNK9 – The Human Protein Atlas). Members of protein family 14-3-3 interact with TASK-3 through the C-termini, and this interaction is essential for assembly and trafficking of TASK channel proteins to the surface membrane (Rajan et al. 2002), whereas activation of Gαq mediated pathway is believed to inhibit the channel (Mathie 2007; Veale et al. 2007).

At the cellular level, TASK-3 determines background potassium conductance and resting membrane potential. Studies on TASK-3 knockout mice have demonstrated that granule neurons exhibit depolarized membrane potentials with substantially disfigured action potential generation (Brickley et al. 2007; Enyedi and Czirják 2010). Studies investigating TASK-3 channel variants in humans have identified various electrophysiological effects. These effects include both outwardly and inwardly rectifying currents, with some variants exhibiting significantly increased or reduced currents compared to wildtype controls. Additionally, certain variants show currents that are indistinguishable from those observed in wildtype individuals, depending on the affected amino acids (Cousin et al. 2022).

Additionally, TASK-3 has been shown to contribute to higher-level functions, such as cognition, mental retardation, depression, and sleep, and it has effects on pharmacological sensitivity to anaesthesia (Borsotto et al. 2015). Mutations in the *kcnk9* gene have been associated with KCNK9 imprinting syndrome, also referred to as Birk-Barel syndrome. This rare genetic disorder, with only 47 known cases reported worldwide (Cousin et al. 2022), affects neurodevelopment and leads to a range of symptoms including intellectual disabilities, delays in motor and speech development, sleep disturbances, and behavioural abnormalities.

In our present study, we investigated the role of TASK-3 in the suprachiasmatic nucleus (SCN) and its contribution to regulating and maintaining stable cellular and behavioural entrainment. We used a global TASK-3 knockout animal model to assess the impact of TASK-3 on the circadian regulation of cellular excitability and photoentrainment. Our findings demonstrate that TASK-3 plays a role in maintaining SCN

neuronal homeostasis, ensuring stable daily electrical output and robust behavioural responses to light, but it is not necessary for day-to-day functioning.

Materials and methods

Animals

The generation of TASK-3 mice can be found in Brickley et al. (2007). Initial breeders for TASK-3 knockout (KO) line were gifted by William Wisden. Mice for behavioural and molecular work were bred on a C57BL/6J background from heterozygous parents generating TASK-3 KO and littermate wildtype (WT) animals. In behavioural experiments, adult male mice (2–10 months old) were housed individually in polypropylene cages with food and water available *ad libitum*.

P16–23 male and female pups were used in all electrophysiology experiments. Because of the young age, genotyping would be difficult to perform before recordings, so TASK-3 knockout mice were bred from homozygous parents and WT C57BL/6J were used as controls in these *in vitro* studies.

All behavioural testing was performed at Charles River Animal Facility (UK, Margate) using infrared sensors (LuNAR™ PIR 360°, Risco Group) or 8 cm internal diameter cardboard running wheels (specified in the figure legend). The data was collected using The Chronobiology Kit (Stanford Software systems). Activity counts per minute were recorded, and data was saved to the computer every hour.

All procedures complied with the UK Animals (Scientific Procedures) Act (1986) and were performed under a UK Home Office Project License in accordance with University of Oxford and University of Kent Policy on the Use of Animals in Scientific Research. This study conforms to the ARRIVE guidelines.

Electrophysiology

All electrophysiology recordings and analyses were undertaken as previously described using 320 μm coronal slices containing SCN (Lalic et al. 2020). Coronal slices containing SCN were prepared in ice-cold high-sucrose artificial cerebrospinal fluid (aCSF) after decapitation under isoflurane anaesthesia. Slices were then transferred to oxygenated aCSF (95% O₂/5% CO₂) containing 130 mM NaCl, 25 mM NaHCO₃, 2.5 mM KCl, 1.25 mM NaH₂PO₄, 2 mM CaCl₂, 1 mM MgCl₂ and 10 mM glucose and then allowed to rest at room temperature until recording. Cells were typically visualised from 30 to 100 μm below the surface of the slice. Resting membrane potential (RMP) was

measured immediately upon establishing whole-cell access. RMP and spontaneous firing were recorded in bridge mode while zero current was inputted (I = 0 mode).

Breeding, experimental setup, and recordings from TASK-3 KO animals were undertaken as part of a study that included TRESK-KO mice and their relevant control animals. As the breeding and slice preparation protocols for these in vitro experiments limited the use of littermate controls, we have used the appropriate WT animals which reflect the background of both our TASK-3 and TRESK KO lines. All the experiments were done at the same time for all genotypes and were performed by the same individual. Therefore, we have used this WT data to compare against our TASK-3 KO electrophysiology recordings (this manuscript) as well as against already published TRESK KO data (Lalic et al. 2020).

Extracellular action potential recordings using microelectrode arrays

SCN slices were placed on a microelectrode array (MEA) with 256 electrodes arranged in a 16 × 16 grid with inter-electrode distance of 100 μm. Signals from all electrodes were collected simultaneously using the USB-256MEA acquisition system (Multichannel Systems, Germany). Two-minute recordings were collected and repeated three times at 20 kHz. Channels within the SCN were identified visually, and spontaneous extracellular action potential recordings from these SCN channels were discriminated offline using threshold-based event counting through custom written scripts in IgorPro. Thresholds were typically set at 3.5× the baseline noise level, with typical signal amplitude between 20 and 75 μV. Single unit discrimination was not routinely possible in these experiments. Inactive electrodes were excluded in the analysis. Data was only excluded if there was an error when undertaking a given protocol, otherwise no data was excluded.

Drugs

L-Glutamic acid was purchased from Tocris Bioscience. Drugs were added to oxygenated aCSF to final concentration immediately before use.

To assess the effect of glutamate on MEA activity of acute SCN slices, we bath applied different concentrations of glutamate (0, 10, 30 and 100 μM) with recording commencing 5 min after starting perfusion and continuing for 2 min. The same slice was used with successively increasing concentrations of glutamate. Glutamate application and recordings were done at Zeitgeber time (ZT)

12–18. Data was analysed using repeated measures design.

Locomotor activity during light-dark (LD) and dark-dark (DD) housing

Behavioural testing was performed at Charles River Animal Facility (UK, Margate) using the infrared sensors. WT and TASK-3 KO males were individually housed under 12:12 LD cycles, and environmental lighting was provided using LED strips fitted above each row of cages providing equal irradiance to all animals. Twenty-four-hour LD activity profile was plotted by extracting data in 30 min bins over 9–10 days of activity recording (days, when cages were cleaned, were excluded). Mean 24-h activity for each animal was calculated and plotted as mean ± SEM.

For phase angle of entrainment, Actogram Phase Ruler available in the Chronobiology Kit Analysis software was used to measure the time difference (in minutes) between activity onset and the lights off. Activity starting after the lights off was plotted as a negative value (delayed activity onset). For the alpha duration, activity onset and offset were estimated by an eye fit, and activity duration was measured using Actogram Phase Ruler.

For Interdaily stability (IS) and Intradaily variability (IV) assessments, data was extracted in 10 min bins and analysed in Excel. The IS is calculated by dividing the 24-h variance by the overall variance that represents the 24-h value from the chi-square periodogram (Sokolove and Bushnell 1978; Van Someren et al. 1996) using the formula:

$$IS = \frac{N \sum_{h=1}^p (\bar{X}_h - \bar{X})^2}{p \sum_{i=1}^N (X_i - \bar{X})^2} = \frac{N \left((\bar{X}_1 - \bar{X})^2 + (\bar{X}_2 - \bar{X})^2 + \dots + (\bar{X}_p - \bar{X})^2 \right)}{p \left((\bar{X}_1 - \bar{X})^2 + (\bar{X}_2 - \bar{X})^2 + \dots + (\bar{X}_N - \bar{X})^2 \right)} \quad (1)$$

Where N , is the total number of data points, and for a reading every 10 min for 10 d this equals to $6 \times 24 \times 10 = 1440$ data points. The number of data points per day is p , and \sum refers to the sum operator.

Intradaily variability (IV) was calculated using the same data set. It is the frequency of transitions between rest and activity and is calculated by dividing the mean squares of the difference between consecutive hours by the overall variance (Van Someren et al. 1996) as follows:

$$IV = \frac{N \sum_{i=2}^N (X_i - X_{i-1})^2}{(N - 1) \sum_{i=1}^N (\bar{X} - X_i)^2} \quad (2)$$

Free-running behavioural rhythms were measured from animals housed for 10 days of constant darkness following stable entrainment to a LD cycle. Data was extracted in 10 min bins for daily IR beam breaks or in 30 min bins for a daily activity profile. Because *tau* of free-running mice is shorter than 24 h, 11 h of activity after the activity onset (from Circadian Time [CT] 12) and 11 h before the activity onset were used for each animal to plot the daily activity profile for all animals giving 22 h of activity plot (Figure 3C).

Activity profiles were determined by “eye-fitting” regression lines to activity onsets under DD. Each daily intersection along this line determined the activity onset, thus CT 12. From CT 12, $-11/+11$ h of activity data were used to plot the daily profile.

Pupillary light reflex

Pupillometry was conducted as previously described (Biello et al. 2018; Lalic et al. 2020) on unanaesthetised 2–8 month old male and female mice ($n = 8$ per genotype). Animals were stably entrained to a 12:12 h LD cycle (white fluorescent source, 350 lux), and recordings were restricted to between 4 and 8 h after lights on (ZT 4–8). All experiments were preceded by 1 h of dark adaptation. Pupillary responses were elicited with xenon arc lamp (OptoSource High Intensity Arc, Cairn Research) whole spectrum white light stimuli filtered with neutral density filters. Light stimulus was applied to one eye, allowing pupil constriction of another eye to be recorded with a CCD camera (Best Scientific, Swindon) every 0.3 s. Pupillary images were taken for 3 s in the dark followed by 60 s of image recording with light stimulus. Pupil area was measured using ImageJ (National Institutes of Health (NIH), USA) analysis software. To plot the irradiance response curve, the most constricted area of the pupil (min) for each animal was divided by the most dilated area (max) obtained during recording in darkness giving a normalized pupil area.

Circadian pacemaker resetting with a light pulse

All the phase shifting experiments were undertaken following at least seven days of stable entrainment and using the Aschoff type II protocol. Individually housed male mice were entrained to a 12:12 LD cycle with 400 lux illumination during the light period. Five-minute 400 lux light pulses were administered at CT 6, ZT 14 or ZT 18. During the light pulse, all mice remained in their home cages. On the day of the light pulse (for light pulses administered at ZT 14 and ZT 18), mice were placed under constant conditions of darkness and for

animals receiving CT 6 light pulse, the lights were turned off from the previous day ZT 12. After light pulses, mice were left to free-run for a minimum of ten days before data collection and analysis.

For measuring changes in light sensitivity under bright light housing conditions, mice were kept under 2000 lux light for 4 weeks before the ZT 14 2000 lux 5-min light pulse.

To quantify the effect of light pulse on c-fos levels in the SCN, we used the same protocol for ZT 14 5-min 2000 lux light pulses for animals housed under 400 lux light and collected the brains at ZT 15.5. To administer the light pulse, mice were moved in their home cage to a light tight box where they received a light pulse. For the control animals, they were moved to a light tight box too and were kept in it for 5 min with no light on.

Immunohistochemistry

Following a sham or a 2000 lux light pulse in WT and TASK-3 KO mice ($n = 3$ mice per group) at ZT 14, mice were culled using cervical dislocation at ZT 15.5 and their brains were submerged in an ice-cold 4% PFA for 24 h at 4°C. The samples were cryoprotected in 30% sucrose-PBS solution at 4°C until the brains sunk to the bottom of a falcon tube. They were then embedded into a cryoblock using OCT tissue-freezing medium, flash frozen in a -80°C ethanol bath, and subsequently stored at -80°C . For each brain, 60 μm thick coronal sections were cut and used for immunohistochemistry.

Free-floating brain sections containing SCN underwent heat-mediated antigen retrieval in citrate buffer (10 min at 90°C , pH6), followed by cooling to room temperature. Sections were then immersed in blocking solution (PBS, 0.1% triton-X, 5% donkey serum) for 1 h at room temperature before incubation with primary cFOS antibody (Proteintech 66 590-1-Ig, 1:500) for 48 h at 4°C. After primary incubation, sections were washed in PBS, followed by incubation with donkey anti-mouse-Alexa Fluor 594 (Invitrogen, A-21203, 1:500) secondary antibody. After 90 min room temperature incubation with secondary antibody, the sections were washed with PBS and incubated with DAPI (1 $\mu\text{g}/\text{ml}$ in PBS) for 20 min at room temperature. Sections were washed in PBS before securing on to polysine coated slides and mounting with ProlongTM Glass antifade (ThermoFisher Scientific, P36982). Images were obtained using a Zeiss LSM880 confocal microscope using Zen Blue software. ImageJ software was used to analyse images. Z-stacks were combined and mean cFOS fluorescence intensity recorded from SCN regions manually selected using a closed polygon tool.

Re-entrainment (phase shifting to advanced lighting cycle)

WT and TASK-3 KO male mice were housed individually under IR motion sensors using 400 lux light illumination, unless stated otherwise. After stable entrainment, the LD cycle was advanced by 6 h resulting in a shortened light period on the day of the LD shift. Animals were maintained under the new LD cycle until full re-entrainment was reached, defined by at least seven days of stable entrainment. Data was analysed by measuring activity advance relative to baseline for each animal, each day of recording for 12 days using Actogram Phase Ruler on The Chronobiology Kit software. Results were then analysed using repeated measured design.

Statistical analysis

Data are represented as means \pm SEM (unless specified otherwise), and “n” refers to the number of observations. Comparisons for statistical significance were assessed by either a one-way ANOVA, two-way ANOVA or t-test. The Kolmogorov-Smirnov non-parametric test was conducted if the data was found not to pass normality tests. Differences were considered significant if $p < 0.05$. The data was plotted and analysed using GraphPad Prism version 9.

Results

Loss of TASK-3 abolishes diurnal variation in resting membrane potential (RMP) and dampens SCN's endogenous cellular electrical firing rhythm and glutamate sensitivity

Both the ablation of TASK-3 or mutations in this ion channel have been shown causes electrophysiological changes (Brickley et al. 2007; Cousin et al. 2022; Enyedi and Czirják 2010). We first wanted to assess what happens to circadian clock neurons in absence of TASK-3. Recordings from WT SCN neurons were found to display a diurnal variation in membrane potential, with RMP at -48 mV during the day and -56.9 mV during the night ($p = 0.002$, Tukey's multiple comparisons test). However, in the absence of TASK-3, this diurnal variation was abolished, and the SCN RMP resided at -48 mV regardless of time of day ($p = 0.99$, Figure 1A). Comparison between genotypes revealed that TASK-3 KO neurons are significantly more depolarized during the night ($p = 0.0014$). Two-way ANOVA showed a significant variance between genotypes ($F_{(1, 57)} = 6.5$, $p = 0.01$), time of the day ($F_{(1, 57)} = 7.8$, $p = 0.007$) and overall data interaction ($F_{(1, 57)} = 8.6$, $p = 0.005$).

We then examined spontaneous SCN firing activity using freshly prepared coronal SCN slices on multi-electrode arrays with 100 μ m spacing between the electrodes. Mean firing rate (MFR) measurements taken from SCN cells during the day reveal significantly dampened daytime firing rate in TASK-3 KO's compared to WT ($p < 0.0001$, two-way ANOVA with Tukey's multiple comparisons test, Figure 1B). The source of variation is significant for genotype ($F_{(1,1762)} = 37.2$, $p < 0.0001$), time of the day ($F_{(1,1762)} = 92.8$, $p < 0.0001$) and overall interaction between the datasets ($F_{(1,1762)} = 31$, $p < 0.0001$, two-way ANOVA). We found the SCN neurons in TASK-3 KO's to be significantly silenced during the day ($p < 0.0001$) compared to WT daytime levels with respect to MFR. However, the difference between day and night-time firing rates, within genotypes, remained significant ($p < 0.0001$ for WT and $p = 0.02$ for TASK-3 KO).

To assess the effect of TASK-3 loss on light transduction mechanisms during the night, we applied glutamate, the neurotransmitter responsible for relaying light input from the retinohypothalamic tract to the SCN (Suppl. Figure S1). Glutamate was added to freshly prepared SCN slices, and recordings were performed in the early night (ZT 12–18). Analysis of data skewness through their quartiles and probability density shows a concentration-dependent increase in firing rate in a population of WT neurons. In addition, neurons above the 75th percentile responded with highly elevated firing across all glutamate concentrations (Figure 1C). In contrast, SCN cells from TASK-3 knockout (KO) mice did not exhibit such dose-dependent effects as neurons above the 75th percentile did not show a gradual increase in firing (Figure 1C). As the data did not pass normality tests, we performed a nonparametric Kolmogorov-Smirnov test which showed a significant difference between genotypes in the firing rates following the application of glutamate at concentrations of 10 μ M, 30 μ M and 100 μ M ($p < 0.00001$).

To compare changes in firing differences within the genotype, we performed a Tukey's multiple comparisons test. As all the firing rate data was normalized to the baseline, we could directly assess the effect of glutamate on the firing rate. The highest firing rate change in WT SCN neurons was observed with 100 μ M glutamate application, which was significantly higher compared to 10 μ M and 30 μ M glutamate-induced firing ($p < 0.0001$ for both comparisons). However, there was no difference between 10 μ M and 30 μ M glutamate-induced firing ($p = 0.08$). Surprisingly, TASK-3 KO results showed a significant difference in firing rate between 10 μ M and 30 μ M glutamate ($p < 0.0001$), but no difference between 30 μ M and 100 μ M glutamate application ($p = 0.6$).

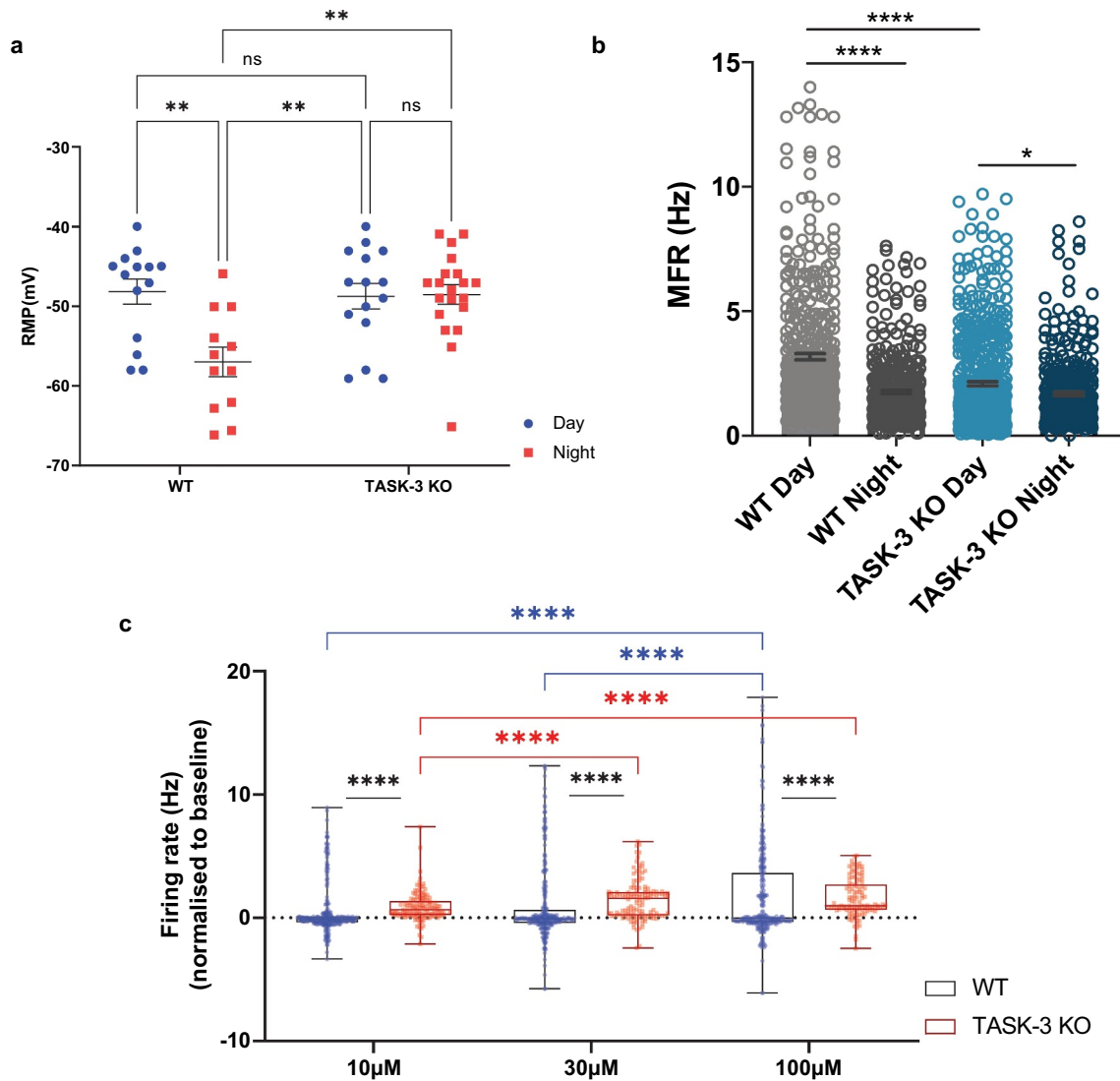


Figure 1. The role of TASK-3 in SCN firing. (A) Whole-cell, current clamp recordings of SCN neurons during the subjective day/night from WT and TASK-3 KO mice. TASK-3 KO mice lack diurnal variation in RMP, remaining in a constantly depolarized state. WT: day $n = 14$, night $n = 12$; TASK-3 KO: day $n = 15$, night $n = 20$ (n is the number of recorded cells). (B) Mean firing rate (MFR) in WT SCN shows diurnal variation, with significantly higher MFR levels during the day. This was significantly dampened to WT night levels in TASK-3 KO mice. MFR calculated by pooling data from all SCN electrodes (WT; day, $n = 7$; night, $n = 8$ animals; TASK-3 KO; day, $n = 5$; night $n = 5$ animals). (C) In vitro glutamate application on acute SCN slices: Box plots from WT mice show a wide distribution in firing rate above 75th percentile, but this is lost in TASK-3 KO mice. The difference in firing rate was significant between genotypes at all tested glutamate concentrations. Only WT animals showed significant increase in firing after 100 μM compared to 30 μM glutamate. Data is normalized to baseline firing rate. * $p < 0.05$, ** $p < 0.01$, *** $p < 0.001$, **** $p < 0.0001$. Data presented as mean \pm SEM. The WT data in A–C is reused from Lalic et al. (2020) paper as explained in the methods.

Loss of TASK-3 results in increased nocturnal locomotor activity

Locomotor activity was assessed in male mice using cage-fitted infrared sensors. Wildtype and TASK-3 KO animals housed under a 12:12 light–dark cycle showed stable synchronized activity profiles (Figure 2A,B). However, TASK-3 KO animals exhibited elevated activity during the later night (Figure 2C). The two-way ANOVA showed significance between genotypes ($F_{(1,576)} = 37.7$, $p < 0.0001$), time of the day ($F_{(47,576)} = 26.3$, $p < 0.0001$) and the overall data

interaction ($F_{(47,576)} = 2.4$, $p < 0.0001$). Bonferroni's test between genotypes revealed a significant difference in activity levels at ZT 18.5, 20 and 21.5. The overall 24 h infrared beam breaks were significantly elevated in the knockout mice; in line with previously published work (Linden et al. 2007; Figure 2D, $p = 0.006$, Student's t-test). Knockout animals showed a significant delay in phase angle of entrainment (Figure 2E, more negative values mean more delay, $p = 0.011$, unpaired t-test), but there were no differences in alpha duration, interdaily

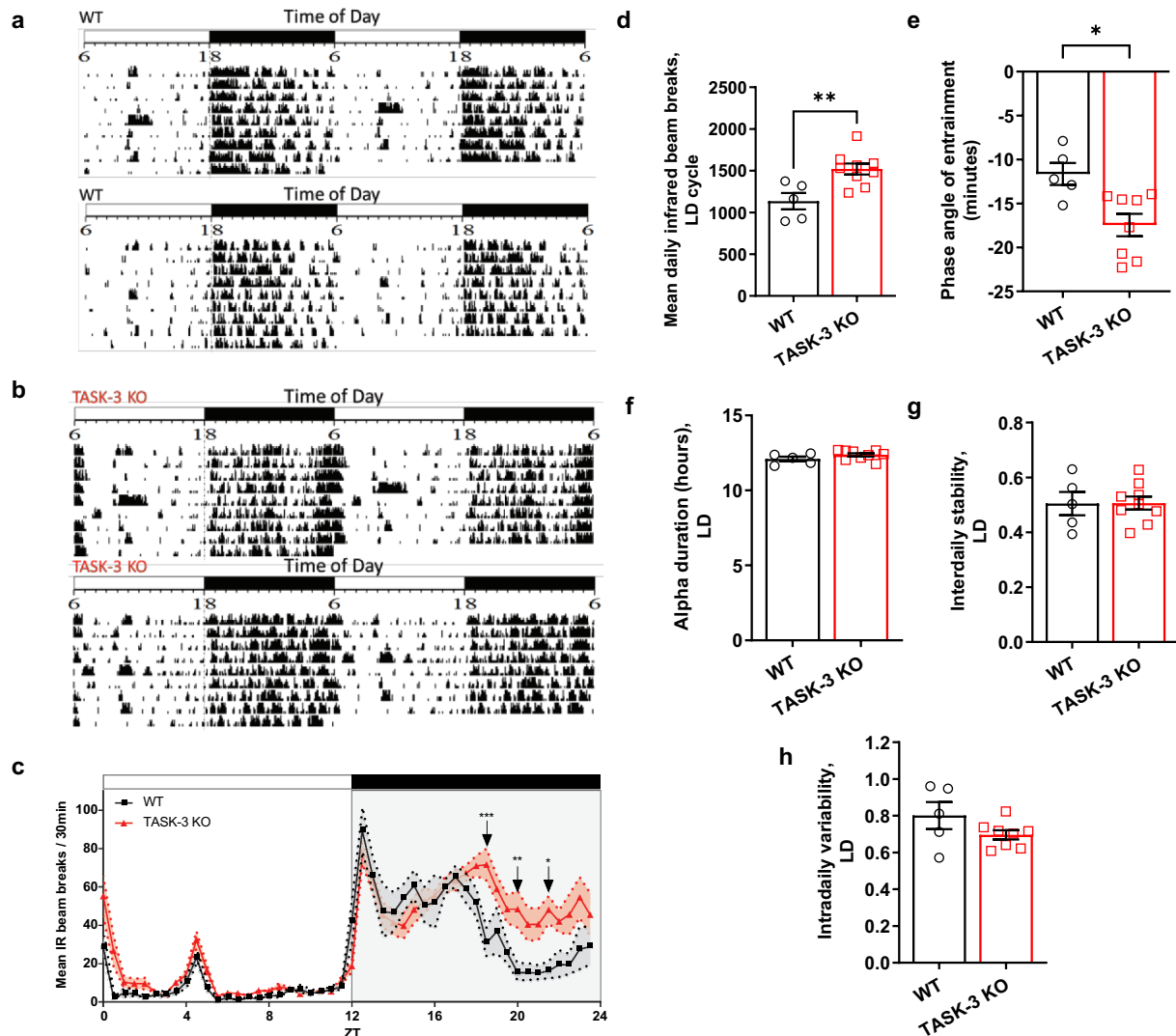


Figure 2. Locomotor activity under 12:12 LD cycle. Infrared beam break recordings under 12:12 LD show higher TASK-3 KO activity. (A) Representative actograms from WT and (B) TASK-3 KO mice. (C) TASK-3 KO animals have significantly increased locomotor activity in the second half of the night, with significantly higher overall 24-hour activity (D). Knockout animals have significant delays in phase angle of entrainment (E), but no changes in alpha duration (F), interdaily stability (G) and intradaily variability (H). Pairwise comparisons done using unpaired t-test and 24-h profiles analysed using two-way ANOVA with Bonferroni's test. $n = 5$ WT, 9 KO. * $p < 0.05$, ** $p < 0.01$, *** $p < 0.001$. Shaded areas in C represent SEM, data presented as mean \pm SEM.

stability or intradaily variability (Figure 2F-H). To eliminate changes in the retinal decoding of light, we have assessed the pupillary light reflex under white light (Supplementary Figure S2). Pupil constriction was not affected at the tested light intensities (10^{13} – 10^{16} photons/cm²/s) which overlapped in the relative irradiance of the room illumination under which all of our behavioural experiments were performed. Therefore, the observed behaviour differences are not likely due to any retinal alterations in sensitivity to light in TASK-3 KO mice.

Housing animals under constant conditions of darkness showed free-running rhythms to be maintained in both WT and TASK-3 KO animals (Figure 3A–C). However, the differences in overall activity remained under such

environmental conditions. Two-way ANOVA showed a significant variation between genotypes ($F_{(1,528)} = 46$, $p < 0.0001$), time of the day ($F_{(43,528)} = 28.3$, $p < 0.0001$) and overall interaction ($F_{(43,528)} = 1.9$, $p = 0.0009$). TASK-3 KO mice showed significantly higher activity at CT 17, 21, 21.5 and 22 – the latter portion of the night. The sum of daily infrared beam breaks remained significantly higher in knockout animals (Figure 3D, $p = 0.02$, Student's t-test). However, no differences were found between genotypes in the alpha duration (Figure 3E), period length (23.81 ± 0.025 hr and 23.83 ± 0.025 hr, respectively), interdaily stability (Figure 3F) or intradaily variability (Figure 3G).

As leak potassium channels are mainly active in the SCN during the night, we tested circadian *Task-3* mRNA

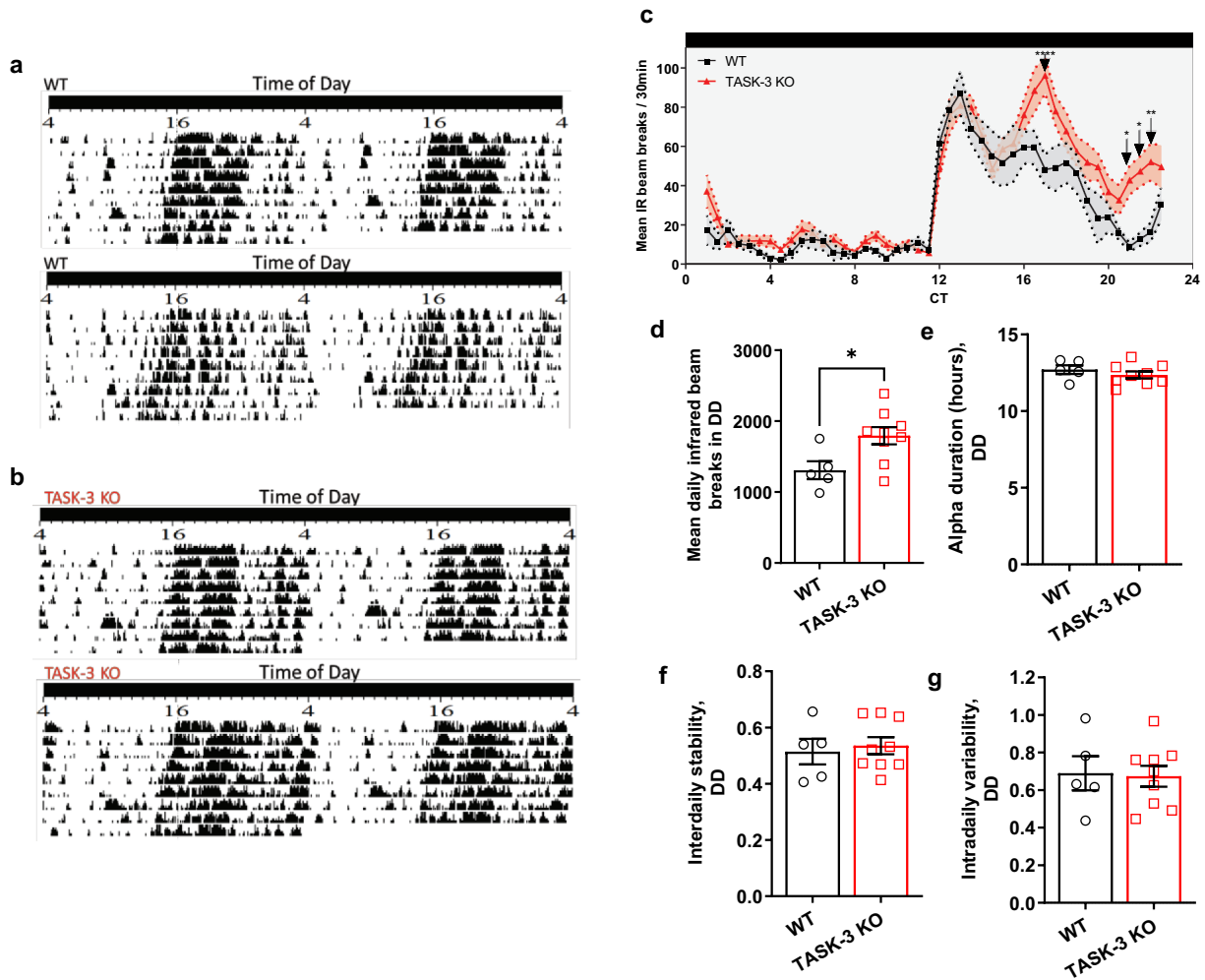


Figure 3. Locomotor activity under constant darkness (DD). (A) Representative actograms from WT and (B) TASK-3 KO mice housed in constant darkness. Activity recordings in constant darkness show that TASK-3 KO mice remain significantly more active between CT 16–22 (C) and their overall activity is significantly higher than in WT (D). There are no changes in alpha duration (E), interdaily stability (F) and intradaily variability (G). Pairwise comparisons done using unpaired t-test and 24-hour profiles analysed using two-way ANOVA with Bonferroni's test. $n = 5$ WT, 9 KO. * $p < 0.05$, ** $p < 0.01$, *** $p < 0.001$. Shaded areas in C represent SEM, data presented as mean \pm SEM.

expression and found that the highest mRNA levels were during the middle of the night (Supplementary Figure S3).

TASK-3 facilitates the attunement of circadian behavioural responses to acute light stimuli

To assess the impact of TASK-3 loss in circadian behavioural resetting, we administered brief light pulses during the middle of the day, early and late night (CT 6, ZT 14 and ZT 18 respectively). A 5-min 400 lux light pulse induced a phase shift at ZT 14 and 18 but this was not different between genotypes (Figure 4A, Supplementary Figure S4, two-way ANOVA with Tukey's multiple comparisons test; genotype $F_{(1,35)} = 1.8$, $p = 0.2$, data interaction $F_{(2,35)} = 0.7$, $p = 0.5$, time of day $F_{(2,35)} = 23.4$, $p < 0.0001$).

We then tested light intensity-dependent effects on phase shifting. In wildtype mice, administering increasing intensity light pulses at ZT 14, two hours after the lights turn off, results in higher phase delays, especially after a 2000 lux light pulse (Figure 4B, Supplementary Figure S5). However, in mice lacking TASK-3, phase delays did not differ between the different intensity light pulses, and the phase shift after a 2000 lux light pulse was significantly smaller compared to WT ($p = 0.012$, Tukey's multiple comparisons test). Two-way ANOVA showed that the source of variation is significant for genotype ($F_{(1,48)} = 7.7$, $p = 0.008$), light pulse intensity ($F_{(2,48)} = 9.4$, $p = 0.0004$) and overall data interaction ($F_{(2,48)} = 3.2$, $p = 0.05$).

Having seen that a 2000 lux light pulse did not result in significantly greater phase shift in TASK-3 KO

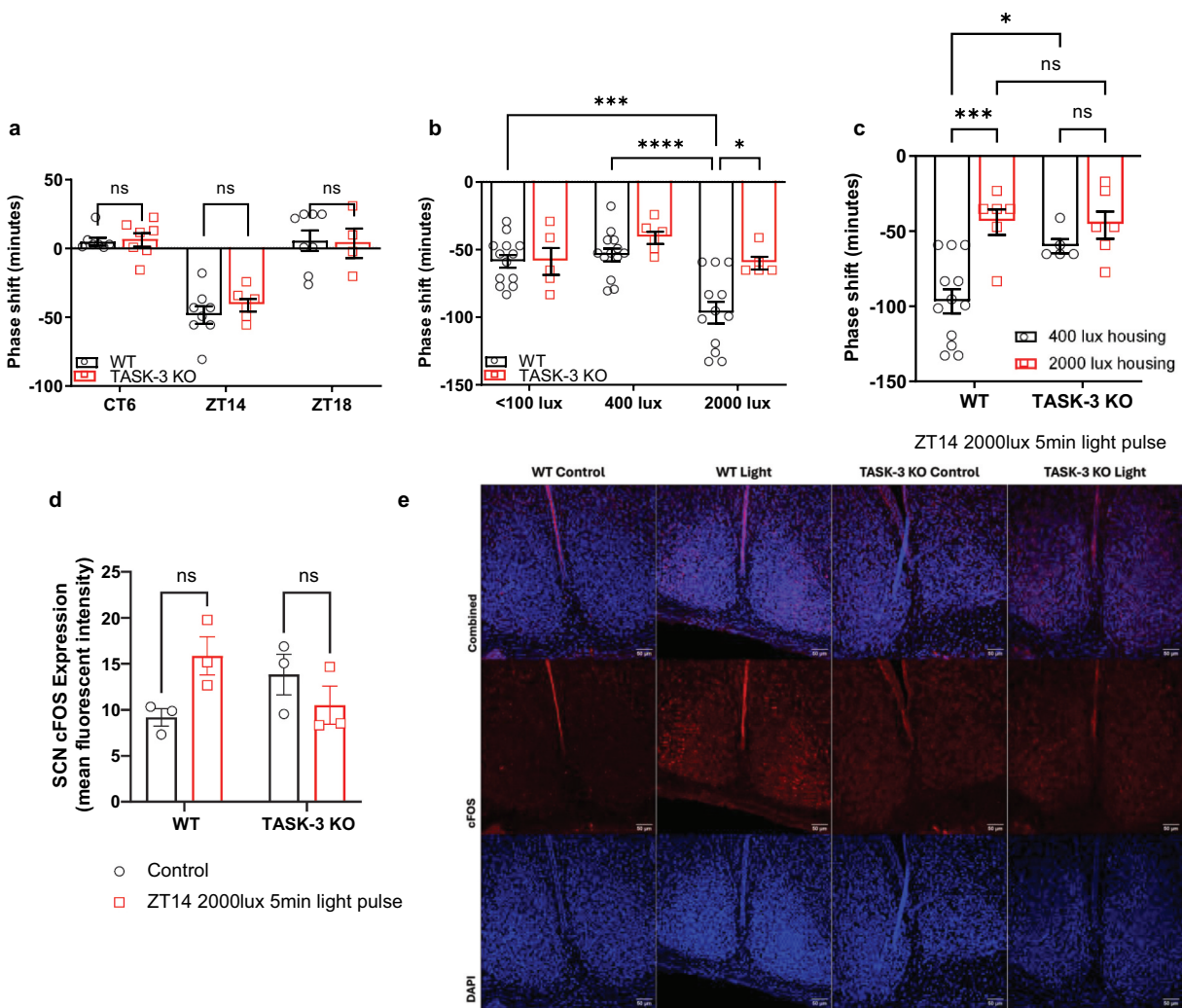


Figure 4. Acute responses to light and re-entrainment to 6-hour advanced LD cycles (jet-lag paradigm). (A) 5 min light pulses (400 lux) presented in the middle of the day (CT6: $n = 7$ WT/KO) or early/late night (ZT 14: $n = 8$ WT, 6 KO; and ZT 18: $n = 8$ WT, 4 KO) resulted in phase delays with no differences between genotypes. (B) A 5 min light pulse administered at ZT 14 showed intensity depended phase delaying effects in behavioural activity in wild type mice however this was absent on TASK-3 KO animals ($n = 13$ WT, 5 KO). (C) 5 min 2000 lux light pulse at ZT 14 after ambient (400 lux) and high light intensity (2000 lux) housing showed decrease in WT phase shift, but no differences in TASK-3 KO phase shift because of bright light housing. (D) cFOS expression in the SCN measured by using closed polygon tool to outline SCN region based on DAPI staining. Light pulse resulted in c-FOS increase in WT, but not TASK-3 KO sections. (E) Representative examples from c-FOS staining showing combined, c-FOS only and DAPI only sections across four tested groups. Sections were imaged using 20 \times objective and the scale bar represents 50 μm . A–D -Two-way ANOVA with Tukey's multiple comparisons test, * $p < 0.05$, ** $p < 0.01$, *** $p < 0.001$, **** $p < 0.0001$, data presented as mean \pm SEM.

animals when compared to tested lower intensities, we wanted to assess whether the circadian system becomes desensitized to light stimulus during bright light housing. Therefore, we housed animals under 2000 lux light-dark cycle for 4 weeks before administering ZT 14 2000 lux light pulse for 5 min (Figure 4C, Supplementary Figure S6). As expected, WT animals exhibited significantly reduced phase delays in response to 2000 lux light pulses when housed under 2000 lux light compared to 400 lux housing ($p = 0.0007$, Tukey's multiple comparisons test). However, in TASK-3 KO mice, we observed

no significant difference in phase shifts between the two experiments, and the magnitude of the phase shift was comparable to the delays observed in WT mice housed under bright light conditions. The two-way ANOVA showed significant variations due to housing light intensity ($F_{(1,25)} = 13.2$, $p = 0.0013$) and overall data interaction ($F_{(1,25)} = 4.4$, $p = 0.05$).

To better understand light-induced effects at a protein level, we stained SCN containing coronal sections after administering a 5-min 2000 lux light pulse to animals housed under 400 lux light and compared the results to

no-light controls (Figure 4D,E). Similarly to what we observed in behavioural responses, WT mice had a greater increase in c-FOS expression, although this difference was not significant ($p = 0.1367$, Tukey's multiple comparisons test). Interestingly, we saw a decrease in c-FOS levels after the light pulse in TASK-3 KO mice ($p = 0.6221$). Two-way ANOVA showed a significant levels of interaction between genotype and light treatment ($F_{(1,8)} = 6.944$, $p = 0.0299$), but there were no significant differences between genotypes or light pulse treatment only ($F_{(1,8)} = 0.035$, $p = 0.8563$ and $F_{(1,8)} = 0.7829$, $p = 0.4026$, respectively).

Thus far, we tested acute responses to light. However, in order to assess the impact on chronic light entrainment we exposed our animals to a re-entrainment protocol ("jet-lag," Figure 5A,B). Therefore, to evaluate the impact of TASK-3 on stable photoentrainment of the circadian clock system, we exposed animals to a 6-h advance in the light-dark cycle, and measured the daily activity shift compared to the baseline activity onset (Figure 5C). Knockout mice showed significantly higher variability in re-entrainment patterns, with higher variance than in WT mice since day 2 (Suppl. Fig. S7, overall variance 0.18 ± 0.26 for WT and 0.53 ± 0.7 for TASK-3 KO, Mean \pm SD). However, both genotypes took a similar number of days to reach re-entrainment. Mixed-effects analysis showed no overall significant differences between genotypes ($p = 0.8$), but a significant

interaction between hours of phase advance on different days since the phase shift and the genotype ($p = 0.0064$). Bonferroni's multiple comparisons test showed that phase advance between genotypes was only significant on day 2 ($p = 0.005$).

Considering the changes observed in acute bright light pulse effects to phase shifting when animals were housed under different light intensities, we assessed the impact of 2000 lux light-dark cycles on rates of re-entrainment. Re-entrainment to a 6-h advance in the light-dark cycle did not show any differences between genotypes in any of the post light advance days (Suppl. Fig. S8A), but this time WT animals showed greater variance in the hours shifted for each day (Suppl. Fig. S8B). The comparison of re-entrainment rate across different light intensities used for housing the animals showed that WT and TASK-3 KO adjusted quicker to the new advanced light-dark cycle when housed under 400 lux light (Suppl. Fig. S9A and B). It was also evident that bright light housing resulted in higher variance in rates of re-entrainment in WT animals (0.64 ± 0.58) compared to TASK-3 KO (0.19 ± 0.14) when measured across all 13 d of data (Suppl. Figure S9C).

Discussion

We have shown that TASK-3 leak two-pore domain potassium channels play an important role in regulating

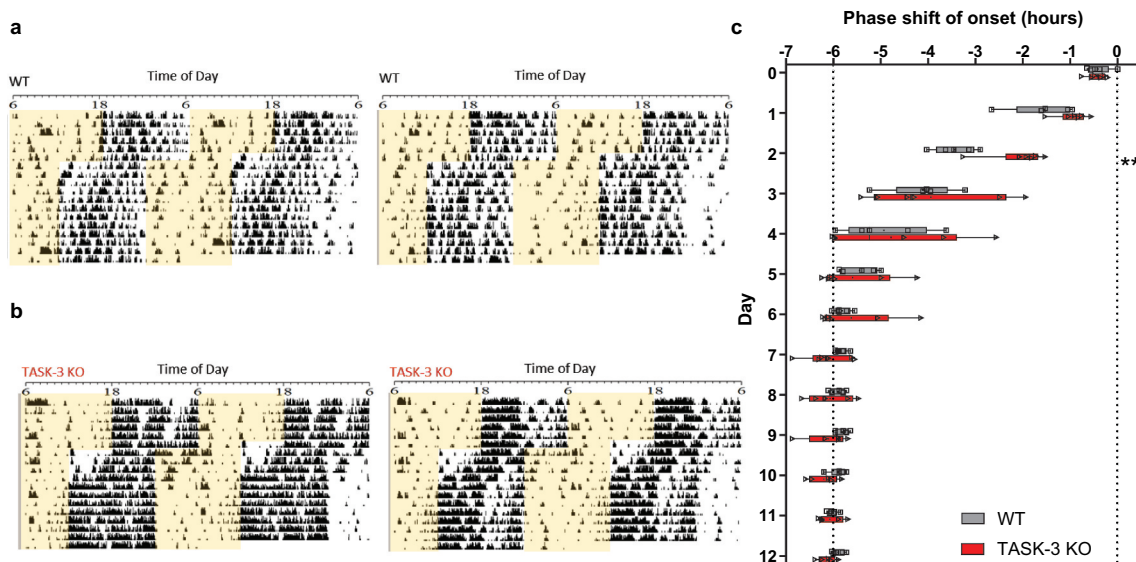


Figure 5. Re-entrainment to 6-h advanced LD cycles (jet-lag paradigm). (A) Representative 6-h re-entrainment actograms from WT and (B) TASK-3 KO mice. (C) Following a 6-h advance in the light-dark cycle during 400 lux light housing, both genotypes took the same number of days to re-entrain to the new environmental conditions, but TASK-3 KO mice had more varied bouts of activity some given days indicated by the spread of the daily box plots. In particular, the rate of re-entrainment was significantly different on day 2 ($n = 5$ WT, 6 KO). C – repeated measures mixed-effects analysis with Bonferroni's multiple comparisons test. $**p < 0.01$, data presented as mean \pm SEM.

electrical properties of the SCN and subsequently behavioural responses to light. Our findings suggest that the loss of TASK-3 results in a dampened diurnal firing rate and impaired sensitivity to glutamate in a dose-dependent manner, indicating an altered circadian regulation of cellular excitability.

TASK-3 is needed for maintaining high diurnal mean firing rates in SCN neurons and for lowering resting membrane potential at night. Interestingly, the day and night RMP in the TASK-3 KO mice reside at the same level as that of the wildtype daytime. Thus, this would imply that the SCN in these transgenic animals remains in a - constant day-like state with regards to RMP. It is already known that SCN neurons show day-night differences in the RMP and, as a result, reduction in the firing rate at night, with two-pore potassium channels being heavily involved in nightly silencing (Colwell 2011). Therefore, we had expected to see a reduction in nightly hyperpolarization in absence of TASK-3 yet were surprised that this effect was present to the extent that there was a complete loss in diurnal RMP differences. However, the link between resting membrane and excitability is often complex. Intuitively, one might envisage that loss of a hyperpolarizing brake at night (in this case TASK-3 activity) might increase excitability and therefore firing rates, as mentioned by (Harvey et al. 2020). But we have found that the spontaneous MFR maintained day-night variation, although the firing rate was dampened in the SCN; most likely due to the inability of neurons to reset rapidly in the absence of TASK-3 (Brickley et al. 2007). Furthermore, despite RMP showing a daytime state during the night in these mice, it is possible that the reduced nighttime MFR is due to the natural reduction of overall spontaneous activity, driven primarily by large-conductance Ca^{2+} activated K^+ (BK) channels as well as other members of K2P family (Colwell 2011). Another possibility could centre around changes in cellular membrane input resistance, which are partially facilitated by K2P channels. K2P channels have been shown to mediate nocturnal silencing of SCN neurons, also supported by our findings showing a significant decrease in the MFR in WT SCN neurons (Harvey et al. 2020). With the loss of TASK-3, the input resistance facilitated by other K2P channels may still be present, but not to the same extent as in WT. Therefore, the degree at which MFR rate at night is suppressed in TASK-3 KO mice may be reduced. Future studies into this area would be beneficial.

Behaviourally, we found little evidence of impact to daily activity profiles beyond those previously reported by Linden et al. (2007) showing increased locomotor activity during the night. This also correlates with previous findings that TASK-3 KO animals display a severe

decrease in sleep duration (Yoshida et al. 2018). Interestingly, we found that knockout animals have significantly reduced “siesta” period in the late portion of the night resulting in overall higher night-time activity. It is possible that this may be linked to the changes we saw in the dampened diurnal firing rate. Research has shown that a quarter of all recorded units in the SCN are the most active during the siesta period and most of the siesta-active neurons are VIPergic siesta-specific neurons (Collins et al. 2020). In addition, acute exposure to constant light causes arrhythmicity in VIP neurons and silencing SCN VIP neurons cause attenuated responses to light-induced shifts. If knocking out TASK-3 affects VIPergic siesta-specific neurons, there would be changes in light-mediated resetting of the circadian system, which is highly controlled by SCN VIP neurons (Jones et al. 2018). Furthermore, the dampened diurnal firing rate amplitude may cause a wider phase distribution of the SCN single cell neuronal activity within the network (Ramkisoensing and Meijer 2015). This could explain increased delays in the phase angle of entrainment and reduced ZT 14 light induced phase shifting effects in TASK-3 KO mice – as arrhythmic neurons would have less robust outputs.

Having established the importance of TASK-3 in maintaining the electrical properties of SCN neurons, we turned our attention to investigating the impact of this channel in driving the input of cellular communications. Glutamate, an excitatory neurotransmitter, mediates light signals to the SCN (Ginty et al. 1993; Michel et al. 2002). To assess the effect of glutamate application on SCN neurons, we applied glutamate *in vitro* to the SCN of TASK-3 KO mice and observed cellular excitation that was similar at lower (30 μM) and higher (100 μM) concentrations, with fewer neurons showing a dose-dependent increase in firing, particularly in the data above the 75th percentile. Our behavioural experiments showed a corresponding decrease in phase shifting to bright light in TASK-3 KO mice, similar to the dose-response effect observed with glutamate. One prediction could be that TASK-3 KO mice should exhibit an increase in phase shifts to light given their heightened sensitivity to glutamate. However, this was not the case and suggests that other post-glutamatergic signalling pathways may be impacted in these mice. Given the role of these channels in resting membrane potential resetting, it could be possible that the lack of TASK-3 is preventing repeated firing and thus reducing signal strength, especially at high glutamate doses and light levels. Interestingly, the phase shifting magnitudes were unaffected by environmental housing light intensities (ambient or bright) in TASK-3 KO animals, while data from WT mice suggested that neurons may become

desensitized to the effects of glutamate during bright light housing. This might be explained by depolarization block – bright light might result in higher levels of glutamate release silencing some neurons (Meijer et al. 1993).

Although we initially hypothesized that TASK-3 would play a more significant role in acute phase shifting to light, our findings indicate that its impact is more pronounced under extreme environmental lighting conditions. In a re-entrainment paradigm, we observed that mice lacking TASK-3 exhibited greater variability in tracking the dawn signal, particularly during the first few days following the advancement of a light–dark cycle. If our hypothesis on the changes to SCN VIP neurons due to the knocking out of TASK-3 is correct, it would explain the higher variability in rates of re-entrainment across animals, as the SCN would be more arrhythmic compared to WT mice. Furthermore, during the first few days of re-entrainment following a 6-h advance in the light–dark cycle, the light turns on at a time when the body clock is at CT 18. Light during the night would normally result in increased VIP neuronal activity and VIP release, which is needed for efficient response to light (Jones et al. 2018). However, as discussed earlier, mice lacking TASK-3 may experience alterations in SCN VIP neurons, potentially leading to changes in daily re-entrainment rate and genotype differences during the first few days of the light advance period, when the circadian system is most out of synchrony with the environment.

When advancing light–dark cycles with 2000 lux light during the day, no differences were observed between genotypes in the re-entrainment rate, a result that matches light pulse-induced phase shifting after bright light housing. However, if bright light housing indeed causes depolarization block in some neurons (Meijer et al. 1993), this could delay SCN resetting, and it would take animals longer to re-entrain. Furthermore, greater arrhythmicity in SCN VIP neurons because of TASK-3 deletion and light exposure during the subjective night (when the body's clock is at CT 18) during the first few days after phase advance would mean that both genotypes have higher SCN desynchrony, thereby explaining no differences in re-entrainment during bright light housing.

It was interesting to see that TASK-3, in our hands, convincingly impacts the electrical properties of the SCN, however, it has less prominent effects on behavioural output. It is possible that the dampened MFR in TASK-3 KO mice leads to an overall reduced electrical coupling between internal SCN regions as well as

efferent targets, thus hindering SCN cell-to-cell communication. This would lead to SCN neurons unable to effectively synchronize, and whilst they can respond to a stimulus (such as a light pulse or direct glutamate application), the magnitude and efficiency of the response is variable when compared to their wildtype counterparts. The SCN possesses a vast array of ion channels that allow and facilitate the conveying of external stimuli to clock cells and further allow cell-to-cell communication. Table 1 illustrates an array of key ion channels that have been found to impact both electrophysiological and behavioural properties of circadian timing. Removing particular ion channels can be lethal, for instance, in the case of NALCN or $\text{Na}_v1.1$ (Han et al. 2012; Lu et al. 2007). Less profound, but nevertheless significant circadian changes have been shown by the absence of calcium-activated K^+ channel BK ($\beta 2$ subunit), Fast delayed rectifier (FDR) potassium channels $\text{Kv} 3.1$ and 3.2 as well as two-pore domain (K2P) TRESK channels, all of which impact the electrical properties of the SCN and their respective knockouts show significant effects to light-induced clock resetting when compared to wildtype animals (Kudo et al. 2011; Lalic et al. 2020; Whitt et al. 2016).

One of the limitations of our current work is the use of a global TASK-3 knockout. While a global knockout may aid in understanding gene function in the body and shed light on diseases resulting from specific mutations, such as Birk Barrel's syndrome, there is a risk of off-target effects and compensation mechanisms. TASK-3 has been shown to be present in astrocytes and microglia (Gnatenco et al. 2002; Kim et al. 2011; Rusznák et al. 2004), and it is known that astrocytes play a crucial role in driving circadian behaviour (Brancaccio et al. 2019). Therefore, the results we present here might be due to a combination of various factors affected by globally knocking out TASK-3. Thus, further studies would benefit from a more targeted conditional KO model. In addition, we also note that our electrophysiology data sets were recorded from slices taken from mouse pups. It may be beneficial to extend the study into using slices from older maturer animals, however viability of the preparations can be variable.

Overall, our study highlights the role of TASK-3 leak two-pore domain potassium channels in regulating the electrical properties of SCN neurons and their impact on behavioural responses to light. Our results indicate that a deficiency in TASK-3 channels can cause a disruption in the circadian regulation of cellular excitability, resulting in decreased diurnal firing rates and reduced sensitivity to glutamate. These changes can ultimately lead to altered

Table 1. The role of major ion channels on the electrical properties of SCN neurons and circadian behavioural activity.

Ion channel	Animal KO survival	Changes in RMP	Changes in MFR	Impact on locomotor activity and responses to light	Published works
NALCN Nav1.1	Die within 24 h of birth HOM mice die at P15, but HET live	N/A N/A	N/A • ↓ neuronal excitability	N/A • Longer free-running in DD • Activity under LD and DD housing, peak activity later in the night • No phase shift after light pulse at CT16 • Slow re-entrainment to 6-h advance and delay • Faster re-entrainment to 6-h advance, • ↑ Phase delay to CT16 light pulse • ↑ Daytime activity, • ↓ Phase shifts at CT16, • Some animals arrhythmic under LD and DD housing • ↑ Day time locomotor activity (but not overall activity levels), • Normal free-running, • ↓ Sensitivity to light pulses at CT14 and glutamate induced firing	Lu et al. (2007) Han et al. (2012)
BK (β2 subunit)	YES	N/A	• ↓ firing amplitude and rhythmicity, • no difference in day vs night firing rate • ↓ spontaneous activity during the day (to the night time levels), • ↓ NMDA response at night		Whitt et al. (2016)
FDR (Kv 3.1, 3.2)	YES	N/A			Kudo et al. (2011)
K2P (TREK)	YES	• ↓ diurnal variation, • Night time depolarisation (same as day time)	• Dampened day time firing, • ↓ day vs night difference		Lalic et al. (2020)

behavioural responses to light, including reduced phase shifting to bright light and increased variability in re-entrainment to a new light–dark cycle.

Acknowledgments

We would like to thank Charles River (UK) for the daily care of animals. This study has received support from the Innovative Medicines Initiative Joint Undertaking under grant agreement n°115439, resources of which are composed of financial contribution from the European Union’s Seventh Framework Programme (FP7/2007–2013) and the Royal Society (RG100842).

Disclosure statement

M.Z.C. reports personal fees from Eli Lilly, Novartis and grants from Orion, Daiichi Sankyo, and Oxford Science Innovations outside the submitted work.

Funding

This study has received support from the Innovative Medicines Initiative Joint Undertaking under grant agreement no. 115439, resources of which are composed of financial contribution from the European Union’s Seventh Framework Programme (FP7/2007–2013) and the Royal Society (RG100842).

References

Allen CN, Nitabach MN, Colwell CS. 2017. Membrane currents, gene expression, and circadian clocks. *Cold Spring Harb Perspect Biol.* 9:1–16. doi: [10.1101/cshperspect.a027714](https://doi.org/10.1101/cshperspect.a027714).

Biello SM, Bonsall DR, Atkinson LA, Molyneux PC, Harrington ME, Lall GS. 2018. Alterations in glutamatergic signaling contribute to the decline of circadian photoentrainment in aged mice. *Neurobiol Aging.* 66:75–84. doi: [10.1016/j.neurobiolaging.2018.02.013](https://doi.org/10.1016/j.neurobiolaging.2018.02.013).

Borsotto M, Veyssiere J, Moha Ou Maati H, Devader C, Mazella J, Heurteaux C. 2015. Targeting two-pore domain K⁺ channels TREK-1 and TASK-3 for the treatment of depression: a new therapeutic concept. *Br J Pharmacol.* 172:771–784. doi: [10.1111/bph.12953](https://doi.org/10.1111/bph.12953).

Brancaccio M, Edwards MD, Patton AP, Smyllie NJ, Chesham JE, Maywood ES, Hastings MH. 2019. Cell-autonomous clock of astrocytes drives circadian behavior in mammals. *Science.* 363:187–192. doi: [10.1126/science.aat4104](https://doi.org/10.1126/science.aat4104).

Brickley SG, Aller MI, Sandu C, Veale EL, Alder FG, Sambhi H, Mathie A, Wisden W. 2007. TASK-3 two-pore domain potassium channels enable sustained high-frequency firing in cerebellar granule neurons. *J Neurosci.* 27:9329–9340. doi: [10.1523/JNEUROSCI.1427-07.2007](https://doi.org/10.1523/JNEUROSCI.1427-07.2007).

Collins B, Pierre-Ferrer S, Muheim C, Lukacsovich D, Cai Y, Spinnler A, Herrera CG, Wen SA, Winterer J, Belle MDC, et al. 2020. Circadian VIPergic neurons of the

- suprachiasmatic nuclei sculpt the sleep-wake cycle. *Neuron*. 108:486–499.e5. doi: [10.1016/j.neuron.2020.08.001](https://doi.org/10.1016/j.neuron.2020.08.001).
- Colwell CS. 2011. Linking neural activity and molecular oscillations in the SCN. *Nat Rev Neurosci*. 12:553–569. doi: [10.1038/nrn3086](https://doi.org/10.1038/nrn3086).
- Cousin MA, Veale EL, Dsouza NR, Tripathi S, Holden RG, Arelin M, Beek G, Bekheirnia MR, Beygo J, Bhambhani V, et al. 2022. Gain and loss of TASK3 channel function and its regulation by novel variation cause KCNK9 imprinting syndrome. *Genome Med*. 14. doi: [10.1186/s13073-022-01064-4](https://doi.org/10.1186/s13073-022-01064-4).
- Enyedi P, Czirájk G. 2010. Molecular background of leak K⁺ currents: two-pore domain potassium channels. *Physiol Rev*. 90:559–605. doi: [10.1152/physrev.00029.2009](https://doi.org/10.1152/physrev.00029.2009).
- Feliciangeli S, Chatelain FC, Bichet D, Lesage F. 2015. The family of K2P channels: salient structural and functional properties. *J Physiol*. 593:2587–2603. doi: [10.1113/jphysiol.2014.287268](https://doi.org/10.1113/jphysiol.2014.287268).
- Ginty DD, Kornhauser JM, Thompson MA, Bading H, Mayo KE, Takahashi JS, Greenberg ME. 1993. Regulation of CREB phosphorylation in the suprachiasmatic nucleus by light and a circadian clock. *Science*. 260:238–241. doi: [10.1126/science.8097062](https://doi.org/10.1126/science.8097062).
- Gnatenco C, Han J, Snyder AK, Kim D. 2002. Functional expression of TREK-2 K⁺ channel in cultured rat brain astrocytes. *Brain Res*. 931:56–67. doi: [10.1016/S0006-8993\(02\)02261-8](https://doi.org/10.1016/S0006-8993(02)02261-8).
- Han S, Yu FH, Schwartz MD, Linton JD, Bosma MM, Hurley JB, Catterall WA, De La Iglesia HO. 2012. Na V1.1 channels are critical for intercellular communication in the suprachiasmatic nucleus and for normal circadian rhythms. *Proc Natl Acad Sci USA*. 109. doi: [10.1073/pnas.1115729109](https://doi.org/10.1073/pnas.1115729109).
- Harvey JRMM, Plante AE, Meredith AL. 2020. Ion channels controlling circadian rhythms in suprachiasmatic nucleus excitability. *Physiol Rev*. 100:1415–1454.
- Jones JR, Simon T, Lones L, Herzog ED. 2018. SCN VIP neurons are essential for normal light-mediated resetting of the circadian system. *J Neurosci*. 38:7986–7995. doi: [10.1523/JNEUROSCI.1322-18.2018](https://doi.org/10.1523/JNEUROSCI.1322-18.2018).
- Kim J-E, Yeo S-I, Ryu HJ, Chung CK, Kim M-J, Kang T-C. 2011. Changes in TWIK-related acid sensitive K⁺1 and -3 channel expressions from neurons to glia in the hippocampus of temporal lobe epilepsy patients and experimental animal model. *Neurochem Res*. 36:2155–2168. doi: [10.1007/s11064-011-0540-0](https://doi.org/10.1007/s11064-011-0540-0).
- Kudo T, Loh DH, Kuljis D, Constance C, Colwell CS. 2011. Fast delayed rectifier potassium current: critical for input and output of the circadian system. *J Neurosci*. 31:2746–2755. doi: [10.1523/JNEUROSCI.5792-10.2011](https://doi.org/10.1523/JNEUROSCI.5792-10.2011).
- Lalic T, Steponenaite A, Wei L, Vasudevan SR, Mathie A, Peirson SN, Lall GS, Cader MZ. 2020. TRESK is a key regulator of nocturnal suprachiasmatic nucleus dynamics and light adaptive responses. *Nat Commun*. 11. doi: [10.1038/s41467-020-17978-9](https://doi.org/10.1038/s41467-020-17978-9).
- Linden A-M, Sandu C, Aller MI, Vekovischeva OY, Rosenberg PH, Wisden W, Korpi ER. 2007. TASK-3 knockout mice exhibit exaggerated nocturnal activity, impairments in cognitive functions, and reduced sensitivity to inhalation anesthetics. *J Pharmacol Exp Ther*. 323:924–934. doi: [10.1124/jpet.107.129544](https://doi.org/10.1124/jpet.107.129544).
- Lu B, Su Y, Das S, Liu J, Xia J, Ren D. 2007. The Neuronal Channel NALCN contributes resting sodium permeability and is required for normal respiratory rhythm. *Cell*. 129:371–383. doi: [10.1016/j.cell.2007.02.041](https://doi.org/10.1016/j.cell.2007.02.041).
- Mathie A. 2007. Neuronal two-pore-domain potassium channels and their regulation by G protein-coupled receptors. *J Physiol*. 578:377–385. doi: [10.1113/jphysiol.2006.121582](https://doi.org/10.1113/jphysiol.2006.121582).
- Meijer JH, Albus H, Weidema F, Ravesloot J-H. 1993. The effects of glutamate on membrane potential and discharge rate of suprachiasmatic neurons. *Brain Res*. 603:284–288. doi: [10.1016/0006-8993\(93\)91249-R](https://doi.org/10.1016/0006-8993(93)91249-R).
- Meredith AL, Wiler SW, Miller BH, Takahashi JS, Fodor AA, Ruby NF, Aldrich RW. 2006. BK calcium-activated potassium channels regulate circadian behavioral rhythms and pacemaker output. *Nat Neurosci*. 9:1041–1049. doi: [10.1038/nn1740](https://doi.org/10.1038/nn1740).
- Michel S, Itri J, Colwell CS. 2002. Excitatory mechanisms in the suprachiasmatic nucleus: the role of AMPA/KA glutamate receptors. *J Neurophysiol*. 88:817–828. doi: [10.1152/jn.2002.88.2.817](https://doi.org/10.1152/jn.2002.88.2.817).
- Patton AP, Hastings MH. 2018. The suprachiasmatic nucleus. *Curr Biol*. 28:R816–R822. doi: [10.1016/j.cub.2018.06.052](https://doi.org/10.1016/j.cub.2018.06.052).
- Rajan S, Preisig-Muller R, Wischmeyer E, Nehring R, Hanley PJ, Renigunta V, Musset B, Schlichthorl G, Derst C, Karschin A, et al. 2002. Interaction with 14-3-3 proteins promotes functional expression of the potassium channels TASK-1 and TASK-3. *J Physiol*. 545:13–26. doi: [10.1113/jphysiol.2002.027052](https://doi.org/10.1113/jphysiol.2002.027052).
- Ramkisoensing A, Meijer JH. 2015. Synchronization of biological clock neurons by light and peripheral feedback systems promotes circadian rhythms and health. *Front Neurol*. 6:138217. doi: [10.3389/fneur.2015.00128](https://doi.org/10.3389/fneur.2015.00128).
- Renigunta V, Schlichthorl G, Daut J. 2015. Much more than a leak: structure and function of K2P-channels. *Pflugers Archiv Eur J Physiol*. 467:867–894. doi: [10.1007/s00424-015-1703-7](https://doi.org/10.1007/s00424-015-1703-7).
- Rusznák Z, Pocsai K, Kovács I, Pór Á, Pál B, Bíró T, Szücs G. 2004. Differential distribution of TASK-1, TASK-2 and TASK-3 immunoreactivities in the rat and human cerebellum. *Cell Mol Life Sci*. 61:1532–1542. doi: [10.1007/s00018-004-4082-3](https://doi.org/10.1007/s00018-004-4082-3).
- Sans N, Petralia RS, Wang Y-X, Blahos J II, Hell JW, Wenthold RJ. 2000. A developmental change in NMDA receptor-associated proteins at hippocampal synapses. *J Neurosci*. 20:1260–1271. doi: [10.1523/JNEUROSCI.20-03-01260.2000](https://doi.org/10.1523/JNEUROSCI.20-03-01260.2000).
- Sokolove PG, Bushell WN. 1978. The chi square periodogram: its utility for analysis of circadian rhythms. *J Theor Biol*. 72:131–160. doi: [10.1016/0022-5193\(78\)90022-x](https://doi.org/10.1016/0022-5193(78)90022-x).
- Sun H, Luo L, Lal B, Ma X, Chen L, Hann CL, Fulton AM, Leahy DJ, Laterra J, Li M. 2016. A monoclonal antibody against KCNK9 K⁺ channel extracellular domain inhibits tumour growth and metastasis. *Nat Commun*. 7:7. doi: [10.1038/ncomms10339](https://doi.org/10.1038/ncomms10339).
- Takahashi JS. 2017. Transcriptional architecture of the mammalian circadian clock. *Nat Rev Genet*. 18:164–179. doi: [10.1038/nrg.2016.150](https://doi.org/10.1038/nrg.2016.150).
- Talley EM, Solorzano G, Lei Q, Kim D, Bayliss DA. 2001. CNS distribution of members of the two-pore-domain (KCNK) potassium channel family. *J Neurosci*. 21:7491–7505. pii. doi: [10.1523/JNEUROSCI.21-19-07491.2001](https://doi.org/10.1523/JNEUROSCI.21-19-07491.2001).

- Van Someren EJW, Hagebeuk EEO, Lijzenga C, Scheltens P, De Rooij SEJA, Jonker C, Pot AM, Mirmiran M, Swaab DF. 1996. Circadian rest-activity rhythm disturbances in Alzheimer's disease. *Biol Psychiatry*. 40:259–270. doi: [10.1016/0006-3223\(95\)00370-3](https://doi.org/10.1016/0006-3223(95)00370-3).
- Veale EL, Kennard LE, Sutton GL, MacKenzie G, Sandu C, Mathie A. 2007. Gα q -mediated regulation of TASK3 two-pore domain potassium channels: the role of protein kinase C. *Mol Pharmacol*. 71:1666–1675. doi: [10.1124/mol.106.033241](https://doi.org/10.1124/mol.106.033241).
- Welsh DK, Takahashi JS, Kay SA. 2010. Suprachiasmatic nucleus: cell autonomy and network properties. *Annu Rev Physiol*. 72:551–577. doi: [10.1146/annurev-physiol-021909-135919](https://doi.org/10.1146/annurev-physiol-021909-135919).
- Whitt JP, Montgomery JR, Meredith AL. 2016. BK channel inactivation gates daytime excitability in the circadian clock. *Nat Commun*. 7:1–13. doi: [10.1038/ncomms10837](https://doi.org/10.1038/ncomms10837).
- Yoshida K, Shi S, Ukai-Tadenuma M, Fujishima H, Ohno R, Ueda HR. 2018. Leak potassium channels regulate sleep duration. *Proc Natl Acad Sci*. 115:E9459–E9468. doi: [10.1073/pnas.1806486115](https://doi.org/10.1073/pnas.1806486115).